

Magnetic and transport properties in $Gd_{1-x}Sr_xCoO_3$ ($x=0.10-0.70$)

X.G.Luo, H.Li, X.H.Chen, Y.M.Xiong, G.Y.Wang, C.H.Wang, W.J.Miao, and X.Li,
 Hefei National Laboratory for Physical Science at Microscale and Department of Physics,
 University of Science and Technology of China, Hefei,
 Anhui 230026, People's Republic of China

(Dated: October 17, 2019)

Magnetic and transport properties of polycrystalline $Gd_{1-x}Sr_xCoO_3$ ($x=0.10-0.70$) are investigated systematically. Cluster-glass magnetism for $x=0.45$ and long-range ferromagnetic order in higher doping level are observed. Transport measurements indicate insulator-like behaviors for the samples with $x=0.30$, and an insulator-metal (IM) transition around $x=0.35$, and metallic behaviors for higher x samples. In contrast to $La_{1-x}Sr_xCoO_3$, the striking feature is that the system reenters insulator-like state for $x=0.60$, and the long-range ferromagnetic order and IM transition take place in samples with higher Sr content. It could be attributed to the enhancement of low-spin state stability for the trivalent Cobalt ions due to the small radius of Gd^{3+} ion.

PACS numbers: 71.28.+d, 71.30.+h, 73.43.Qt

I. INTRODUCTION

To understand peculiar electromagnetic properties of perovskite-type cobalt oxides, $Ln_{1-x}A_xCoO_3$ (Ln = rare earth element, A = alkali earth metal), such as large negative MR,^{1,2,3} cluster-glass magnetism,^{4,5,6,7} spin-state transition^{8,9} and insulator-metal transition induced by doping or temperature,^{10,11} numerous works have been performed by many researchers. One important part of these works is to change Ln^{3+} or A^{2+} , in order to get information of the electronic structure and magnetic states with different ionic radii or hole concentrations.^{4,5,12,13,14,15}

One striking feature for the richness of the physical properties of $Ln_{1-x}A_xCoO_3$, compared to other transition oxides like CMR manganites, nickelates and cuprates, is the presence of the various spin states for trivalent cobalt ions (low-spin LS, $Co^{III}: t_{2g}^6e_g^0$; intermediate spin IS, $Co^{III}: t_{2g}^5e_g^1$; high spin HS, $Co^{3+}: t_{2g}^4e_g^2$) and tetravalent cobalt ions ($LS, Co^{IV}: t_{2g}^5e_g^0$; IS, $Co^{IV}: t_{2g}^4e_g^1$; HS, $Co^{4+}: t_{2g}^3e_g^2$) and the relative narrow energy gap between these spin states. This makes a thermally spin-state transition easily to occur.^{5,16} Recent experimental and theoretical investigations indicate that the spin states are LS and the mixture of IS/LS for tetravalent and trivalent cobalt ions, respectively.^{9,12,17,18,19,20,21,22}

The magnetic and transport properties are related to the spin state of cobalt ions (trivalent and tetravalent) very closely. In $La_{1-x}Sr_xCoO_3$, it has been found that the hole-rich regions are segregated by the insulating hole-poor matrix.^{4,5} The hole-poor matrix mainly consists of nonmagnetic $LS Co^{III}$. Low spin Co^{IV} ions introduced by doped Sr locate within the hole-rich regions.⁵ In low doping range, the hole-rich regions are $Co^{IV} 6Co^{3+}$ clusters trapped around the isolated Sr^{2+} . As x increases, the hole-rich clusters become larger with more than one Co^{IV} (equally one hole), and the covalent bonding would be strong enough to create molecular orbital states and the cobalt ions within these clusters are stabilized in an intermediate-spin configuration $t_{2g}^5(0:5)$.⁵ The ferro-

magnetic exchange interaction and charge conduction in the compositions are mainly realized by the hopping of electrons between two localized t_{2g} configurations.⁵ Especially, as x increases, bands overlap with bands formed by t_{2g} orbitals hybridized with $O 2p$ orbital, and electrons become itinerant, resulting in bulk metallic conductivity.^{5,16,23}

The evolution of the hole-poor and hole-rich regions and the spin-states with hole concentration leads to a complicated magnetic and electronic behaviors. Studies on $La_{1-x}Sr_xCoO_3$ system reveal a rather rich magnetic and electronic phase diagram with doping level: spin-glass for $x < 0.18$, cluster-glass for $0.18 < x < 0.30$ and ferromagnetic behaviors for $x > 0.30$, insulator-like/metallic resistivity, and metal-insulator transition at $x=0.20$, and so on.^{4,5,10,24} Ca- and Ba-doped compounds $La_{1-x}A_xCoO_3$ ($A=Ca$, and Ba) have also been studied intensively.^{25,26}

Besides the La compounds, other important perovskite cobaltites $Ln_{1-x}Sr_xCoO_3$ ($Ln^{3+}=Pr^{3+}, Nd^{3+}, Sm^{3+}, Eu^{3+}, Gd^{3+}$ etc.) also exhibit complex magnetic and electrical properties.^{25,27,28,29,30,31} In this paper, we investigated Sr-doped gadolinium cobaltites systematically. However, most of the work on $Gd_{1-x}Sr_xCoO_3$ was focused on the evolution of crystal structure with Sr doping,^{31,32} magnetic and transport properties in relative high temperatures ($T > 77 K$).^{31,32} The Gd^{3+} ions have different characters from La^{3+} ion, for example: smaller ionic radius than La^{3+} ions, the high magnetic moment with no (L-S) anisotropy ($L=0, S=7/2$),³⁵ in contrast to the nonmagnetic La^{3+} ($L=0, S=0$). Therefore, the contrasting behavior from La compounds should be expected. In fact, some distinct properties from La compounds have been reported in the Gd compounds. In undoped sample $GdCoO_3$, the cobalt ions are in low-spin state below 270 K,³³ while in $LaCoO_3$, a ratio of 50% Co^{3+} to 50% Co^{III} is already stabilized for $110 < T < 350 K$.^{5,34} Especially, no metallic behavior is reported in $Gd_{1-x}Sr_xCoO_3$ system below 300 K so far,^{31,32,35} in

contrast to the metallic resistivity for $x > 0.20$ in La compounds. In this paper, it is found that cluster-glass magnetism for $x = 0.45$ and long-range ferromagnetic order in higher doping level are observed. Transport measurements indicate insulator-like behaviors for the samples with $x = 0.30$, and an insulator-metal (IM) transition around $x = 0.35$, and metallic behaviors for higher x samples. In contrast to $\text{La}_{1-x}\text{Sr}_x\text{CoO}_3$, the striking feature is that the system reenters insulator-like state for $x = 0.60$, and the long-range ferromagnetic order and IM transition take place in samples with higher Sr content. No obvious effect of Gd^{3+} with high magnetic moment on properties was observed except for a strong paramagnetic signal in low temperatures.

II. EXPERIMENT

Polycrystalline $\text{Gd}_{1-x}\text{Sr}_x\text{CoO}_3$ ($x = 0.10-0.70$) samples were prepared through conventional solid-state reaction. The stoichiometric amounts of Gd_2O_3 , SrCO_3 , and Co_3O_4 powders were thoroughly mixed and fired at 1200°C . After that, the mixture was reground, pressed into pellets and sintered at 1200°C for 24 h. This procedure was repeated for three times. In order to get relative homogeneous sample with less oxygen deficiency, the samples then were annealed in the oxygen pressure of 165 atm at 500°C for 48 h. X-ray diffraction (XRD) was performed by Rigaku D/max-A X-Ray diffractometer (XRD) with graphite monochromated $\text{CuK}\alpha$ radiation ($\lambda = 1.5418 \text{ \AA}$) at room temperature. Magnetization measurement was carried out with a superconducting quantum interference device (SQUID) magnetometer (MPMS-5, Quantum Design). The measurements of resistivity were performed using the standard ac four-probe method. The magnetic field was supplied by a superconducting magnet system (Oxford Instruments).

III. EXPERIMENTAL RESULTS

A. XRD patterns

TABLE I: The lattice parameters of $\text{Gd}_{1-x}\text{Sr}_x\text{CoO}_3$.

x	Lattice parameters (Å)			Reduced lattice volume (Å ³)	Crystal symmetry
	a	b	c		
0.10	5.231	5.392	7.458	52.6	Orthorhombic
0.30	5.252	5.389	7.493	53.0	Orthorhombic
0.40	3.793			54.58	Cubic
0.50	3.796			54.73	Cubic
0.60	3.809			55.27	Cubic
0.70	3.816			56.57	Cubic

Figure 1 shows the XRD patterns for $\text{Gd}_{1-x}\text{Sr}_x\text{CoO}_3$ ($x = 0.10-0.70$). In $x = 0.10$ and 0.30 samples, the XRD

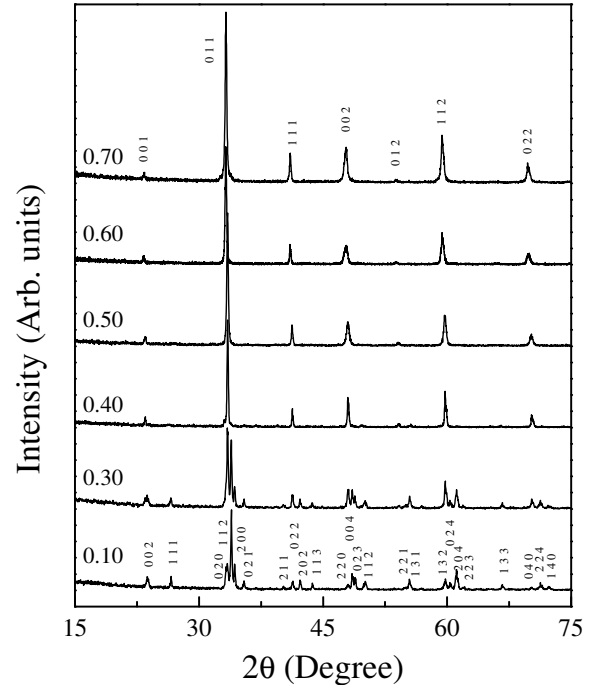


FIG. 1: The XRD patterns of $\text{Gd}_{1-x}\text{Sr}_x\text{CoO}_3$ ($x = 0.10$ to 0.70)

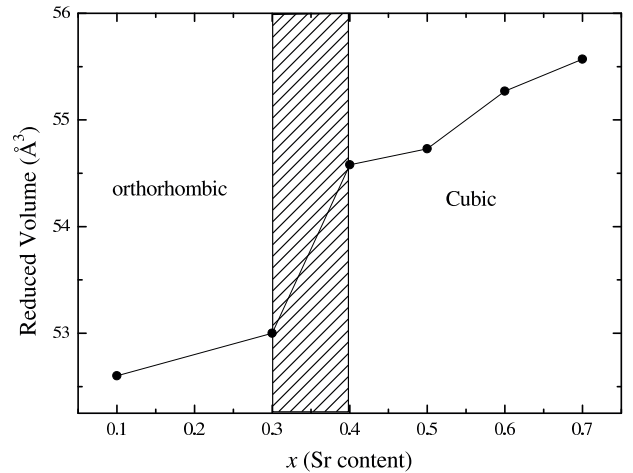


FIG. 2: The reduced volume vs. Sr content in $\text{Gd}_{1-x}\text{Sr}_x\text{CoO}_3$ ($x = 0.10$ to 0.70). The shadow represents the x region with the mixture of orthorhombic and cubic phase.

patterns can be indexed on the basis of a distorted perovskite-type structure with orthorhombic symmetry like GdFeO_3 ,³³ which has been used in the GdCoO_3 (space group, $Pbnm$) with $a_{\text{ort}} = 2a_{\text{per}}$, $b_{\text{ort}} = 2a_{\text{per}}$, $c_{\text{ort}} = 2a_{\text{per}}$.³³ With increasing x , the crystal symmetry changes to be cubic ($Pm\bar{3}m$), in $0.40 < x < 0.70$ samples. The lattice parameters from the Rietveld analysis in GSAS program are shown in Table I. It is found that the lattice parameters in $x = 0.10$ and $x = 0.30$ samples are almost the same as the previous report.³⁵ It

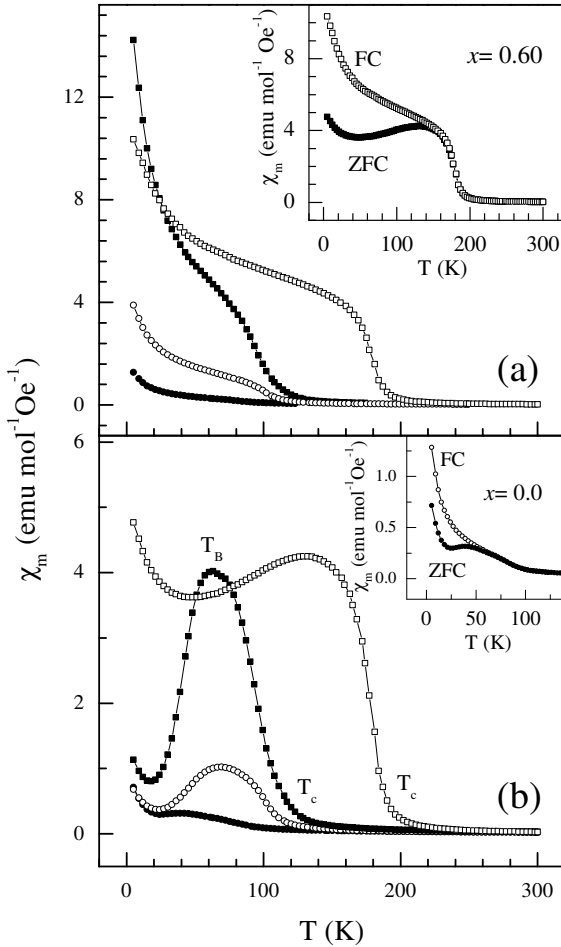


FIG. 3: (a) FC and (b) ZFC molar magnetic susceptibility of $Gd_{1-x}Sr_xCoO_3$ ($x = 0.10$ (\square), 0.30 (\circ), 0.45 (\triangle), and 0.60 (\diamond)) as a function of temperature at $H = 1000$ Oe.

has to be mentioned that some very weak peaks in the XRD data of $x = 0.40$ sample cannot be indexed by cubic symmetry. The very weak un-indexed peaks can be assigned to the orthorhombic phase similar to that in $x = 0.30$ sample. It suggests that there is a little orthorhombic phase mixed with the main cubic phase. Similar phenomena has been reported by Takeda et al.³² They reported the orthorhombic phase for $x = 0.30$, while cubic symmetry for $x = 0.40$, and mixture of orthorhombic and cubic phase for $0.30 < x < 0.40$.³² The reduced volume of unit cell and the crystal symmetry for different x samples are listed in Table I. As shown in Fig. 2, the reduced volume of unit cell increases with the substitution of larger Sr^{2+} ions ($r_{Sr^{2+}} = 1.58$ Å) for smaller Gd^{3+} ions ($r_{Gd^{3+}} = 1.22$ Å).^{36,37}

Figure 3 shows the molar magnetic susceptibility $\chi_m(T)$ plotted against temperature for zero-field cooled (ZFC) and field-cooled (FC) procedures. A pronounced increase in χ_m occurs below a temperature T_c , and the rise becomes more salient with increase Sr concentration. T_c increases slowly for $x = 0.45$ ranging from 95 K in $x = 0.10$ sample to 125 K in $x = 0.45$ sample, consistent with a cluster-glass magnetism. While a remarkable enhancement of T_c takes place as the doping level further increases to $x = 0.60$ with $T_c = 200$ K, indicating that a long-range ferromagnetism may appear. It should be pointed out that T_c of $x = 0.10$ and 0.30 here is much less than that reported by Rey-Cabezudo et al.,³⁵ where T_c is around 160 K. This could be due to different synthesis method of solid state reaction here and "liquid-mix" nitrate precursors method by Rey-Cabezudo et al.³⁵ The different synthesis route may induce some microscopic structure differences, such as the size of crystalline grains. Furthermore, the mixture of crystalline phase observed in the products from solid-state reaction³² is not observed in nitrate precursors method.^{31,35} The different synthesis method may influence the distribution of cobalt ions with different valences, the size of the cluster, and even the interactions between cobalt ions, consequently resulting in the different magnetic transition temperatures in the cluster-glass state.

A rounded maximum appears at the temperatures (T_B) below T_c in the ZFC χ_m curves for $x = 0.1-0.45$ samples. The T_B increases from 39 K in the sample with $x = 0.10$ to 69 K in the $x = 0.30$ sample. This T_B observed in doped perovskite-type cobalt oxides is thought to be the magnetic blocking temperature for superparamagnetic cluster.^{4,5,38,39} Its value increases with x , reflecting the growth of the clusters.³⁵ The magnitude of T_B here is much lower than that reported in Ref.35, 100 K. This difference of T_B could be attributed to the different synthesis route as mentioned above, like T_c . T_B is about 60 K in the $x = 0.45$ sample, slightly less than that in $x = 0.30$ sample. This could be due to the enhancement of the ferromagnetic interaction and the size of ferromagnetic clusters. This can further be evidenced by the behavior of the sample with $x = 0.60$. In this sample, the χ_m behaves like a normal ferromagnet (see the inset of Fig.3 (a)), indicating the presence of a long range ferromagnetic order. With further decreasing T , a rapid increase of χ_m occurs in the low temperatures below T_B . This is considered to arise from the paramagnetic signal of Gd^{3+} .

The $M(H)$ loops at 5 K of these samples are shown in Figure 4. The coercive field and the remanent magnetic moment increase with increasing x , for $x = 0.45$, indicating the growth of the cluster size and the enhancement of the interaction between the clusters. The absence of saturation of $M(H)$ (the inset) in highest field for the sample $x = 0.45$ reflects that the magnetic magnetization comes from the contribution of both magnetically

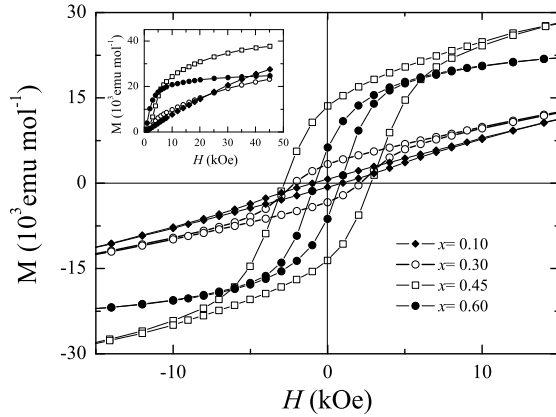


FIG. 4: The $M-H$ loop of $Gd_{1-x}Sr_xCoO_3$ ($x = 0.10$ to 0.60).

ordered cobalt ions ($LS Co^{IV}$ and $IS Co^{III}$) and paramagnetic Gd^{3+} ions. The remarkable increase in the magnitude of magnetic magnetization from $x = 0.10$ to $x = 0.45$ indicates the enhancement of magnetic ordering of the Co ions. It suggests that the ferromagnetic clusters become larger with increasing Sr content. Another feature is that the slope in $M-H$ curve at high fields becomes less with increasing Sr content. It is because the contribution to the susceptibility from the paramagnetic component of the Gd^{3+} decreases with increasing Sr substitution for Gd.

The $M(H)$ curve for $x = 0.60$ sample shows a tendency of saturation in high magnetic fields as shown in the inset of Fig. 4. Combined with the $m(T)$ curves in Fig. 3, it suggests that there exists long range ferromagnetic order in this composition. It should be noted that the coercive field and remanent magnetization in $M(H)$ of $x = 0.60$ become smaller than that in $x = 0.45$. Study on $La_{1-x}Sr_xCoO_3$ system has indicated that the double-exchange interaction between trivalent and tetravalent cobalt spins, and the exchange interaction between low-spin Co^{IV} and intermediate-spin Co^{III} are considered to be ferromagnetic, while the superexchange interactions between the isovalent cobalt ions ($Co^{3+}-Co^{3+}$, $Co^{IV}-Co^{IV}$) are thought to be antiferromagnetic.⁶ The competition between ferromagnetic and antiferromagnetic interactions along with the randomness leads to a spin-glass state in this system for $0 < x \leq 0.18$. As ferromagnetic exchange interactions just overcome the antiferromagnetic one, a cluster glass appears with short range ferromagnetic ordering for $0.18 \leq x \leq 0.50$,⁴ and these clusters are segregated by nonmagnetic insulating Co^{III} matrix. In low doping level, the clusters are separated each other, and they interact each other through the Co^{3+} at the interference of the clusters to the matrix. This interaction is thought to be antiferromagnetic. With increasing the doping level, the clusters become interconnected and the effective interaction between them is fer-

romagnetic. We can apply this picture to $Gd_{1-x}Sr_xCoO_3$ system and to interpret the magnetization effectively. In the sample with $x = 0.10$, the distance between clusters is large, and their interaction is antiferromagnetic and weak. Therefore, small field is needed to align the clusters and small coercive field is observed. With increasing x , the clusters are getting larger and their interaction becomes stronger. It leads to a larger coercive field as observed in $x = 0.30$ and 0.45 samples. As x increases to 0.60 , the clusters become interconnected and the system behaves like a normal ferromagnet. The interaction between clusters is ferromagnetic, so that the coercive field becomes smaller again.

The increase of the remanent magnetization with x less than 0.45 comes from the enhancement of the concentration of tetravalent cobalt ion and the ferromagnetic interaction. At the same time, the contribution from paramagnetic component of Gd^{3+} ions should be considered. One may take into account the Gd^{3+} content to interpret the decrease of the remanent magnetization with increasing x to 0.60 . The saturation of M instead of a linear increase in high magnetic field indicates that the contribution from paramagnetic Gd^{3+} is not significant relative to ferromagnetic component in this sample. Moreover, the contribution of the paramagnetic Gd^{3+} is significant in spin-glass or cluster-glass state for $x \leq 0.45$, so that the Gd content has a strong effect on the magnetization except that one may have to take into account the change of the spin state of the cobalt ions with x .

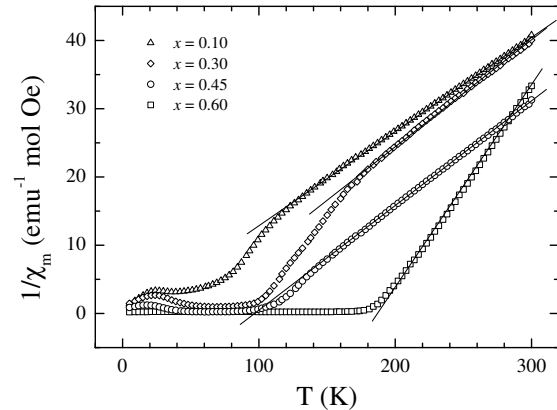


FIG. 5: The inverse ZFC molar magnetic susceptibility plotted against temperature.

Figure 5 shows the $1/\chi_m(T)$ as function of T for the samples with $x = 0.10-0.60$. The $m(T)$ can be fitted to a Curie-Weiss law almost in the temperature range above T_c for $x = 0.45$, and 0.60 samples. While for $x = 0.10$ and 0.30 samples, a strong deviation from the high- T linear $1/\chi_m(T)$ behavior above T_c are observed. In Ref. 35, Rey-Cabezudo et al. have reported that a strong positive deviation from the high- T linearity appears below about 225 K for $x = 0.30$.³⁵ In our case, the deviation

appears below about 175 K, much lower than that in Ref.35. Which is consistent with the lower T_c observed by us than that by Rey-Cabezudo et al.³⁵ It suggests that the different deviation temperature may be related to the magnetic transition. From the fitting result of the corresponding $1/\chi_m(T)$, the effective magnetic moment per cobalt ions μ_{Co} is estimated from the total $\mu_{Co} = \frac{1}{8C}$ after subtracting the Gd^{3+} contribution ($\mu_{Co}(Gd^{3+}) = 7.94 \mu_B$).⁴⁰ The obtained values are $0.59 \mu_B$, $1.75 \mu_B$, $2.96 \mu_B$, and $2.07 \mu_B$ for $x = 0.10, 0.30, 0.45$ and 0.6 samples, respectively. Taking into account the expected effective magnetic moments for trivalent and tetravalent cobalt ions in different spin states ($\mu_{Co_{LS}^{III}} = 0 \mu_B$, $\mu_{Co_{IS}^{III}} = 2.83 \mu_B$, $\mu_{Co_{HS}^{3+}} = 4.91 \mu_B$, $\mu_{Co_{LS}^{IV}} = 1.73 \mu_B$, $\mu_{Co_{IS}^{IV}} = 3.87 \mu_B$, $\mu_{Co_{LS}^{4+}} = 5.91 \mu_B$) and assuming the tetravalent cobalt ions to be low-spin $Co(IV)$ and an intermediate-spin Co^{iii} ,⁵ our results suggest that in $x = 0.10$ and 0.30 samples, most of the cobalt ions are in low-spin state, in agreement with the report by Rey-Cabezudo et al. in Ref.35. Accordingly, by assuming stoichiometric oxygen content, there is 6% and 27% Co^{iii} among all cobalt ions for $x = 0.10$ and 0.30 samples, respectively. For $x = 0.45$ samples, according to the metallic electronic state, a $t_{2g}^5(e_g^0)$ configuration should be considered in an itinerant conduction model. In this case, the spin contribution to the average cobalt ion moment is given by $\mu_{Co} = (x + 2n) \mu_B$, $n = 0.5$ is the number of electrons in the e_g orbital.²⁵ In this way, the effective magnetic moment of cobalt ions per formula is $3.76 \mu_B$, much larger than that obtained from the Curie-Weiss fitting of magnetic susceptibility. This is because in this sample is itinerant and its contribution to local magnetic moment is reduced much. For insulating $x = 0.60$ sample, however, the proportion of intermediate-spin Co^{iii} is reduced to 31%, just a little more than that in $x = 0.30$ sample. This is consistent with the similar transport behavior in $x = 0.30$ and 0.60 samples shown below. According to the effective magnetic moments obtained by fitting $1/\chi_m(T)$ in Curie-Weiss law, the smaller magnetization in $x = 0.60$ sample relative to that in $x = 0.45$ sample can be ascribed to the cooperative effect from the decrease of paramagnetic Gd^{3+} ions and the reduction in quantity of intermediate-spin Co^{iii} .

C. Transport properties

Figure 6 shows the temperature dependence of $\rho(T)$ of the $Gd_{1-x}Sr_xCoO_3$ ($x = 0.10$ to 0.70). The $\rho(T)$ of $x = 0.10$ sample exhibits an insulating behavior in the whole temperature range. With increasing Sr doping level up to 0.45 , $\rho(T)$ decreases dramatically. At 4.2 K, $\rho(T)$ for $x = 0.30$ sample drops by more than 1000 times relative to that of $x = 0.10$ sample, and $\rho(T)$ of $x = 0.45$ sample is reduced by more than 10^5 times relative to that of $x = 0.10$ sample. There exhibits an insulator-metal transition as the Sr content increases up to 0.35 . The $\rho(T)$ of $x = 0.45$ sample is metallic down to 4.2

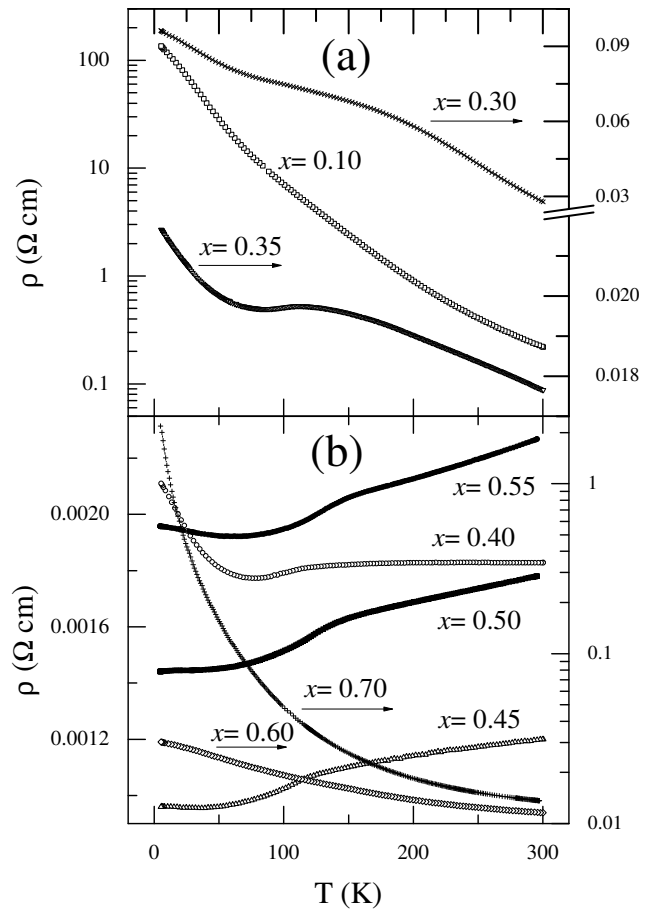


FIG. 6: The temperature dependence of resistivity of $Gd_{1-x}Sr_xCoO_3$ ($x = 0.10$ to 0.70).

K, and shows a kink around 120 K, which is consistent with the ferromagnetic transition temperature. Such a kink of $\rho(T)$ is common feature for an itinerant ferromagnet because the reduction of carrier scattering from spin disorder in ferromagnetic state as observed in CMR manganites⁴¹ and $La_{1-x}Sr_xCoO_3$ ($0.30 < x < 0.60$).⁵ With further increasing Sr content above 0.45 , the $\rho(T)$ increases rapidly. The $\rho(T)$ of $x = 0.50$ sample is still metallic in whole temperature range, while it shows a upturn in low temperatures for $x = 0.55$ sample. It is noteworthy that the position of the kink in $\rho(T)$ shifts to higher temperature with $x = 0.40$ increased to 0.55 , and this is consistent with the enhancement of T_c with increasing x . As Sr content further increases to 0.60 , the resistivity reenters insulating state.

Figure 7 shows the isothermal magnetoresistance at 20 K measured up to 14 T for $Gd_{1-x}Sr_xCoO_3$ with $x = 0.10$, 0.45 , and 0.60 , respectively. The maximum value of the negative MR [$(\rho(H) - \rho(0)) / \rho(0) = -28.5\%$] is achieved in the $x = 0.10$ sample at 13.5 T. The $x = 0.45$ sample, which is the most metallic among all the samples, exhibits a smallest negative MR -6% at 13.5 T. The MR in $x = 0.60$ sample increases to -14% at 13.5 T relative to the $x = 0.45$ sample. This suggests that magnetic

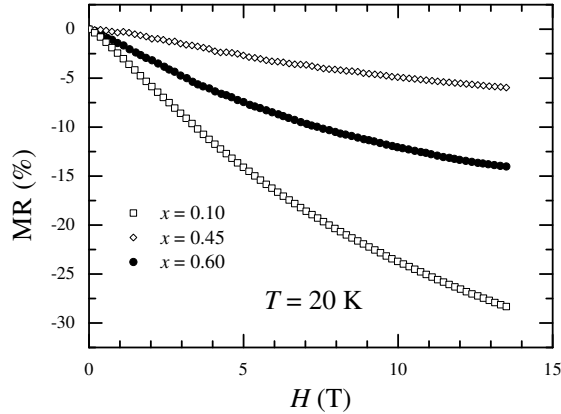


FIG. 7: The isothermal magnetoresistance as a function of magnetic field for $x=0.10$, 0.45 , and 0.60 , respectively.

field has the strongest effect on the most insulating samples. It suggests that the MR depends on not only the ferromagnetic state, but also the insulating state. Similar behavior has been observed in CMR manganites.⁴¹

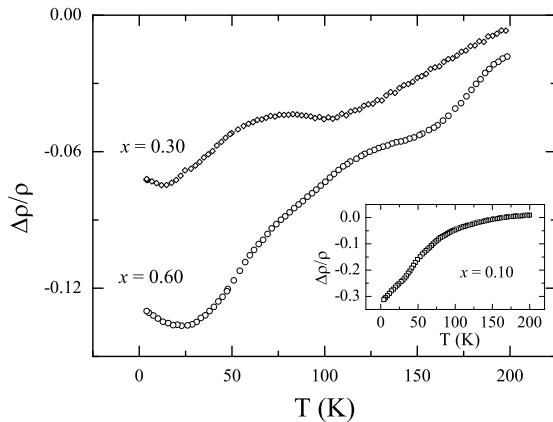


FIG. 8: The temperature dependence of magnetoresistivity of $Gd_{1-x}Sr_xCoO_3$ ($0.10 \leq x \leq 0.60$).

The MR at 13.5 T as a function of temperature for the three insulator-like samples with $x=0.10$, 0.30 , and 0.60 are shown in Fig. 8. The $x=0.10$ sample shows monotonic increase in magnitude with decreasing temperature and has largest value among all the samples. The $x=0.30$ and 0.60 samples show a maximum in the magnitude at low temperature and an anomalous change of slope in high temperature (105 K in $x=0.30$ sample and 165 K in $x=0.60$ sample, respectively), which is consistent with the T_c in the corresponding sample.

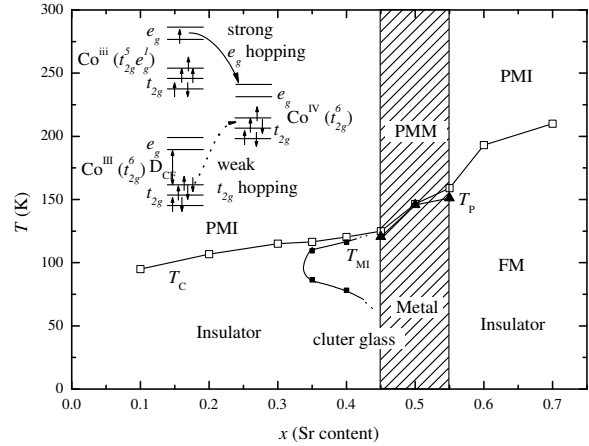


FIG. 9: The schematic drawing of the phase diagram of the $Gd_{1-x}Sr_xCoO_3$ ($0.10 \leq x \leq 0.70$) system. T_c (□): from ac susceptibility; T_p (▲): from resistivity. Shadow represents the region with metallic resistivity ($d\rho/dT > 0$). FM: ferromagnet. PMI/PM: paramagnetic insulator/metal. Inset: possible hopping procedure between trivalent cobalt ions and Co^{IV} . ϵ_{CF} : the energy of crystal field splitting.

IV. DISCUSSION

Figure 9 shows the phase diagram of $Gd_{1-x}Sr_xCoO_3$ ($0.10 \leq x \leq 0.70$) according to the results above. There are some differences between $Gd_{1-x}Sr_xCoO_3$ system and $La_xSr_{1-x}CoO_3$ system.⁵ Firstly, the T_c (200 K) is much less than that in La compounds (250 K). Secondly, the long range ferromagnetic order is achieved as $x > 0.45$ in Gd compounds, while $x \approx 0.30$ in La compounds. Thirdly, the IM transition occurs at $x = 0.35$, in contrast to the $x = 0.20$ in La compounds. Fourthly, the mostly metallic behavior is achieved at $x = 0.45$, while $x = 0.50$ in La compounds. Finally, a striking difference is that the system reenters insulator-like state as $x \approx 0.60$ in Gd compounds. This distinct evolution of magnetic and transport behaviors with x from that in La compounds can be explained with the picture of electrons hopping presented by Thomson et al.⁴² for Ti_2O_3 .

The effect of Gd^{3+} ions on the physical properties of the compounds is mainly due to the smaller ion radius and the higher acidity (i.e. charge/radius ratio) relative to La^{3+} ions ($\chi^{II}_{T_{La^{3+}}} = 1.44 \text{ \AA}$). Recently, Lengsdorf et al.⁴³ reported a transition from the conducting state to an insulating state and a decrease of T_c induced by pressure in $La_{0.82}Sr_{0.18}CoO_3$. This peculiar behavior has been attributed to a gradual change of the spin state of trivalent ions from magnetic to a nonmagnetic spin state under pressure. In $LaCoO_3$, it was found to undergo an intermediate-to-low-spin state transition under pressure.⁴⁴ The change of the spin state with pressure is realized due to the increase in the energy of the crystal-

field splitting (Δ_{CF}) under pressure. The increase of Δ_{CF} makes the low-spin Co^{III} more stable. Gd^{3+} ions have a much smaller radius than La^{3+} ion, therefore, the replacement of Gd^{3+} for La^{3+} has the similar effect like a pressure applied to some extent. It naturally leads to an increase of Δ_{CF} and an enhancement of the stability of the low-spin states than in the La compounds. As observed in GdCoO_3 ,³³ the trivalent cobalt ions are in $\text{Co}(\text{III})$ configuration up to about 270 K, and a ratio of 30% Co^{3+} to 70% $\text{Co}(\text{III})$ is present for $270 < T < 500$ K. While in LaCoO_3 , a proportion of 50% $\text{Co}(\text{III})$ to 50% Co^{3+} is observed for $110 < T < 350$ K, a higher spin configuration is present above 350 K.^{5,34} The effective magnetic moments of cobalt ions obtained just above T_c in Gd compounds are much smaller than that in the La compounds⁵, evidencing the lower-spin configuration in Gd compounds. As presented in Ref.35, the Gd^{3+} ions compete more strongly with cobalt ions in covalent bonding to the oxygen atoms due to the higher acidity than La^{3+} ions. It leads to Co-O bands getting narrower and t_{2g} (Co-O) levels become more stable.⁴⁵ This also causes a more stable low-spin configuration in Gd compounds.

The smaller ion radius and the higher acidity of Gd^{3+} relative to La^{3+} lead to a larger Δ_{CF} , which favors a low-spin Co^{III} . Based on this speculation, the evolution of transport behavior with Sr content can be interpreted as following. According to the model proposed by Goodenough et al.⁵, the conduction is realized by the hopping of t_{2g} electrons (localized or delocalized e_g electrons) from the Co^{III} to the Co^{IV} , as shown in the inset of Fig.9. It shows that it is possible to occur also for the hopping of t_{2g} electrons (t_{2g} electrons) from Co^{III} to t_{2g} orbitals in Co^{IV} . However, the latter has a much smaller possibility to occur than the former one. The gradual increase of higher spin state of trivalent cobalt ions with Sr doping corresponds to an enhancement of the population of the delocalized t_{2g} electrons. It leads to a dramatic decrease of resistivity and finally a metallic state. As discussed above, the larger Δ_{CF} of Gd^{3+} than La^{3+} stabilizes Co^{III} state, so that the IM transition is hindered to occur up to $x = 0.35$ in Gd compounds, a much higher Sr doping level than that ($x = 0.20$) in La compounds. This is why the much larger resistivity is observed in Gd compounds. ($T = 300\text{K}$) $1\text{ m}\Omega\text{cm}$ is observed in Gd compounds, while $0.2\text{ m}\Omega\text{cm}$ in La compounds²⁴ for the corresponding optimal doping composition. The magnetism in perovskite-type cobalt oxide is closely related to exchange interaction between Co^{III} and Co^{IV} , which is thought to be ferromagnetic.^{5,14} The more stable low-spin state of trivalent cobalt ions in Gd compounds than La compounds leads to the occurrence of long range ferromagnetic order up to a critical Sr content higher than $x = 0.45$ in Gd compounds, larger than $x = 0.30$ in La compounds.¹⁰

A metallic resistivity behavior shows up for $x > 0.20$ in La compounds,²⁴ while in the case of Gd compounds, the insulator-like behavior reenters as x increases to 0.60 as

shown in Fig.6. In high Sr doping region, the population of Co^{III} in $x = 0.60$ sample is close to that in the insulating $x = 0.30$ sample, much less than that in the metallic $x = 0.45$ sample. This suggests a reduction in the population of the t_{2g} electrons in $x = 0.60$ sample compared to the most metallic sample with $x = 0.45$. As displayed in the inset of Fig.9, the t_{2g} electrons in Co^{III} are necessary for the charge conduction. Therefore, the reduction of t_{2g} electrons could be considered as possible origin of the insulator-like resistivity as $x = 0.60$.

It has to be pointed out that the conduction through the electron hopping in t_{2g} bands between localized bands is closely related to the Co-O bond-length and Co-O-Co angles. The Co-O-Co angles influence the bandwidth, and overlapping between orbitals of nearest-neighbor Co ions,⁴⁶ and the electronic transfer integral between Co sites.³⁵ The smaller radius of Gd^{3+} ions than that of La^{3+} ions causes a larger distortion from the ideal perovskite structure than the case of La compounds. The smaller Co-O-Co bond angles lead to a reduction of the electronic transfer integral between Co sites, and weakens the itinerate ferromagnetic exchange interaction. Therefore, this is another important reason for the lower T_c , higher critical Sr content for long range ferromagnetic order and for metallic resistivity.

Finally, the large magnetic moment of Gd^{3+} ($S = 7/2$, $\mu_B = 7.94 \mu_B$) should be considered. In this paper, no obvious effect of the magnetic moment of Gd^{3+} on magnetic and transport behavior is observed except for a strong paramagnetic signal observed in low temperatures. Nevertheless, a larger effective field than the applied field on Co ions system can be achieved because the easy orientation of Gd^{3+} sublattice in a magnetic field. Rey-Cabezudo et al.³⁵ pointed out that the paramagnetic Gd^{3+} sublattice polarizes the cobalt magnetic clusters. It has been considered as one possible reason for the low-temperature MR. However, it has been reported that large negative MR (more than 80% at 5 K for $x = 0.09$) was observed in low temperatures for insulator-like compositions of $\text{La}_{1-x}\text{Sr}_x\text{CoO}_3$.²⁴ Considering the fact of the nonmagnetic La^{3+} , the interpretation proposed by Rey-Cabezudo et al. based on Gd^{3+} ions may be in doubt. In Ref. 24, Wu et al.²⁴ interpreted such a negative MR at low temperature in terms of a short-range ferromagnetic ordered cluster model. The Co^{III} and Co^{IV} in the hole-rich clusters are aligned by magnetic field, so that an increase in the electrons hopping possibility results in a negative MR. Therefore, the smallest MR observed in most metallic composition $x = 0.45$ can be understood with the picture proposed by Wu et al. in $\text{La}_{1-x}\text{Sr}_x\text{CoO}_3$ system. It should be pointed out that such low-temperature smallest MR in the most conductive samples is also observed in $\text{La}_{1-x}\text{Sr}_x\text{CoO}_3$ system.²⁴ This indicates that the large negative in low temperature in Gd compounds has the same origin as that in La compounds.

V. CONCLUSION

The evolution of magnetic and transport properties with x in $Gd_{1-x}Sr_xCoO_3$ ($0.10 < x < 0.70$) is investigated systematically. For $x = 0.45$, it exhibits a cluster glass magnetism with T_c changing slightly with x . Larger x results in a long-range ferromagnetic order. Most of the cobalt ions are in low-spin states for $0.10 < x < 0.30$, while for $x = 0.45$, the spin configuration is $t_{2g}^5 e_g^{(0.5)}$ with the itinerant electrons. With further increasing x , the population of $C_{0^{III}}$ decreases dramatically. The resistivity behavior is insulator-like for $x < 0.30$, and an IM transition occurs around $x = 0.35$. The optimal doping is $x = 0.45$. A striking feature is a reentry of insulator-like behavior in the samples with $x = 0.60$. The change of spin states and Co-O-Co bond angles induced by Gd^{3+}

ions are responsible for the distinct behaviors, in contrast to La compounds.

VI. ACKNOWLEDGEMENT

This work is supported by the grant from the Nature Science Foundation of China and by the Ministry of Science and Technology of China (Grant No. nkbbsf-g1999064601), the Knowledge Innovation Project of Chinese Academy of Sciences.

Corresponding author. Electronic address: chenxh@ustc.edu.cn

- ¹ G. Brinceno, H. Chang, X. Sun, P. G. Shulz, and X. D. Xiang, *Science* **270**, 273 (1995).
- ² V. Golovanov, L. Mihaly, and A. R. Moodenbaugh, *Phys. Rev. B* **53**, 8207 (1996).
- ³ R. Mahendiram, and K. Raychaudhuri, *Phys. Rev. B* **54**, 16044 (1996).
- ⁴ M. Itoh, I. Natori, S. Kubota, and K. Motoya, *J. Phys. Soc. Jpn* **63**, 1486 (1994).
- ⁵ M. A. Senaris-Rodriguez and J. B. Goodenough, *J. Solid State Chem.* **118**, 323 (1995).
- ⁶ S. Mukherjee, R. Ranganathan, P. S. Anil Kumar, and P. A. Joy, *Phys. Rev. B* **54**, 9267 (1996).
- ⁷ P. S. Anil Kumar, P. A. Joy, and S. K. Date, *J. Phys. Condens. Matter* **10**, L487 (1998).
- ⁸ S. Mukherjee, P. Raychaudhuri, and A. K. Nigam, *Phys. Rev. B* **61**, 8651 (2000).
- ⁹ N. N. Loshkareva, E. A. Gan'shina, B. I. Belevtsev, Y. P. Sukhorukov, E. V. Mostovshchikova, A. N. Vinogradov, V. B. Krasovitsky, and I. N. Chukanova, *Phys. Rev. B* **68**, 024413 (2003).
- ¹⁰ S. Tsubouchi, T. Kiyomoto, M. Itoh, P. Ganguly, M. Oguni, Y. Shimozu, Y. Mori, and Y. Ishii, *Phys. Rev. B* **66**, 052418 (2002).
- ¹¹ Y. Morimoto, M. Takeo, X. J. Liu, T. Akimoto, and A. Nakamura, *Phys. Rev. B* **58**, R13334 (1998).
- ¹² T. Saitoh, T. Mizokawa, A. Fujimori, M. Abbate, Y. Takeda, and M. Takano, *Phys. Rev. B* **56**, 1290 (1997); T. Saitoh, T. Mizokawa, A. Fujimori, M. Abbate, Y. Takeda, and M. Takano, *Phys. Rev. B* **55**, 4257 (1997).
- ¹³ S. R. Sehlin, H. U. Anderson, and S. M. Sparlin, *Phys. Rev. B* **52**, 11681 (1995).
- ¹⁴ P. Ganguly, M. Hervieu, N. Nguyen, A. Maignan, C. Martin and B. Raveau, *J. Phys.: Condens. Matter* **13**, 10911 (2001).
- ¹⁵ K. Yoshii, H. Abe, and A. Nakamura, *Mater. Res. Bull.* **36**, 1447 (2001).
- ¹⁶ P. M. Raccach, and J. B. Goodenough, *Phys. Rev.* **155**, 932 (1967).
- ¹⁷ M. A. Korotin, S. Y. Ezhov, I. V. Solovyev, V. I. Anisimov, D. I. Khomskii, and G. A. Sawatzky, *Phys. Rev. B* **54**, 5309 (1996).
- ¹⁸ S. Yamaguchi, Y. Okimoto, and Y. Tokura, *Phys. Rev. B* **55**, 8666 (1997).
- ¹⁹ D. Louca, J. L. Sarrao, J. D. Thompson, H. Roder, and G. H. Kwei, *Phys. Rev. B* **60**, R10378 (1999).
- ²⁰ Y. Kobayashi, N. Fujiwara, S. Murata, K. Asai, and H. Yasuoka, *Phys. Rev. B* **62**, 410 (2000).
- ²¹ C. Zobel, M. Kriener, D. Buns, J. Baier, M. Günzinger, T. Lorenz, P. Reutler, and A. Revcolevschi, *Phys. Rev. B* **66**, 020402 (2002).
- ²² P. Ravindran, H. Fjellvåg, A. Kjekshus, P. Blaha, K. Schwarz, and J. Luitz, *J. Appl. Phys.* **91**, 291 (2002).
- ²³ V. G. Bhide, D. S. Rojaria, C. N. R. Rao, G. R. Rao, and V. G. Jadhao, *Phys. Rev. B* **12**, 2832 (1975).
- ²⁴ J. Wu, and C. Leighton, *Phys. Rev. B* **67**, 174408 (2003).
- ²⁵ C. N. R. Rao, O. M. Parkash, D. Bahadur, P. Ganguly, and A. N. Share, *J. Solid State Chem.* **22**, 353 (1977).
- ²⁶ M. Kriener, C. Zobel, A. Reichl, J. Baier, M. Cwik, K. Berggold, H. Kierspel, O. Zabara, A. Freimuth, and T. Lorenz, *Phys. Rev. B* **69**, 094417 (2004).
- ²⁷ H. W. Brinks, H. Fjellvåg, A. Kjekshus, and B. C. Hauback, *J. Solid State Chem.* **147**, 464 (1999).
- ²⁸ A. Fondado, M. P. Beirão, C. Rey-Cabezudo, M. Sanchez-Andujar, J. Mira, J. Rivas, M. A. Senaris-Rodriguez, *J. Alloys Compounds* **323-324**, 447 (2001).
- ²⁹ M. A. Senaris-Rodriguez, M. P. Beirão, S. Castro, C. Rey, M. Sanchez, R. D. Sanchez, J. Mira, A. Fondado, and J. Rivas, *Int. J. of Inorg. Mater.* **1**, 281 (1999).
- ³⁰ D. D. Staurer, and C. Leighton, *Phys. Rev. B* **70**, 214414 (2004).
- ³¹ K. H. Ryu, K. S. Sun, S. J. Lee, and C. H. Yo, *J. Solid State Chem.* **105**, 550 (1993).
- ³² Y. Takeda, H. Ueno, N. Imanishi, O. Yamamoto, N. Sammes, and M. B. Phillips, *Solid State Ion* **86-88**, 1187 (1996).
- ³³ A. Casab, P. Dougier, and P. Hagenmüller, *J. Phys. Chem., Solids*, **32**, 407 (1971).
- ³⁴ M. A. Senaris-Rodriguez and J. B. Goodenough, *J. Solid State Chem.* **116**, 224 (1995).
- ³⁵ C. Rey-Cabezudo, M. Sanchez-Andujar, J. Mira, A. Fondado, J. Rivas, and M. A. Senaris-Rodriguez, *Chem. Mater.* **14**, 493 (2002).
- ³⁶ R. D. Shannon, *Acta Crystallogr. A* **32**, 751 (1976).
- ³⁷ R. D. Shannon, C. T. Prewitt, *Acta Crystallogr. B* **25**, 925 (1969).

- ³⁸ M . A . Senaris-Rodriguez and J . B . G oodenough, *J. Solid State Chem.* **116**, 224 (1995).
- ³⁹ P . G anguly, P . S . A . K um er, P . N . Santhosh, and I . S . M ulla, *J. Phys.:Condens. Matter* **6**, 533 (1994).
- ⁴⁰ A . D ekker, *Solid State Physics*, Prentice-Hall, New York, 1970, p. 450.
- ⁴¹ "Colossal Magnetoresistive Oxides" (Amsterdam 2000), edited by Y . Tokura.
- ⁴² G . Thomton, B . C . To eld, and D . E . W illiam s, *Solid State Commun.* **44**, 1213 (1982).
- ⁴³ R . Lengsdorf, M . A it-Tahar, S . S . Saxena, M . E llerby, D . I . K hom skii, H . M icklitz, T . Lorenz, and M . M . Abd-Elmeguid, *Phys. Rev. B* **69**, 140403 (2004).
- ⁴⁴ T . Vogt, J . A . H riljac, N . C . Hyatt, and P . W oodward, *Phys. Rev. B* **67**, 140401 (2003).
- ⁴⁵ J . B . G oodenough, *Prog. Solid State Chem.* **5**, 145 (1971).
- ⁴⁶ H . Taguchi, *Physica B* **311**, 298 (2002).